Dissolution Behavior of La_2O_3, Pr_2O_3, Nd_2O_3, CaO and Al_2O_3 in Sulfuric Acid Solutions and Study of Cerium Recovery from Rare Earth Polishing Powder Waste via Two-Stage Sulfuric Acid Leaching

Namil Um and Tetsuji Hirato*

Department of Energy Science and Technology, Graduate School of Energy Science, Kyoto University, Kyoto 611-0011, Japan

This study describes a hydrometallurgical process to investigate the cerium recovery from rare earth polishing powder waste (REPPW) containing main elements such as cerium, lanthanum, praseodymium, neodymium, calcium and aluminum. First, dissolution experiments on La_2O_3, Pr_2O_3, Nd_2O_3, CaO and Al_2O_3 with 5 µm particle size in sulfuric acid solutions were carried out using a batch reactor with various acid concentrations (1–15 mol/dm³) at different temperatures (30–180°C). The effects of these two parameters on the dissolution reaction were studied. The obtained results showed that two sequential leaching steps were needed to separate cerium from the mixture of CeO_2, La_2O_3, Pr_2O_3, Nd_2O_3, CaO and Al_2O_3. The total process for cerium recovery from REPPW via two-stage acid leaching was then developed through the collection of experimental results. Moreover, the dissolution rate of Al_2O_3 was expressed by a shrinking core kinetics model. The variation of the dissolution rate constant with temperature obeyed the Arrhenius equation with activation energy of 130 kJ·mol⁻¹ and reaction rate constant as a function of the acid concentration of $C^{0.41}$. On the basis of the above data, a *k-T* (reaction rate constant-reaction temperature) diagram for a CeO_2–Al_2O_3–H_2SO_4–H_2O system that permits rational extraction of CeO_2 and Al_2O_3 was devised.   [doi:10.2320/matertrans.M-M2013802]

1. Introduction

Rare earth metal is now considered the best material in the polishing process because its use has enabled achievement of improved efficiency in industrial polishing processes. Thus, such metals are widely used as polishing powder for glass, semiconductors, or ceramics.[1] After the polishing process, the residue (rare earth polishing powder waste; REPPW) is useless owing to the discharge with polishing liquid or the accumulation of polished components such as aluminum, calcium and silicate materials. According to composition data obtained in previous studies,[1–6] REPPW contains rare earth elements (cerium, lanthanum, praseodymium and neo-dymium) and non-rare earth elements (calcium, aluminum, silicon, barium, magnesium and fluorine) as follows:
Major element: Ce
Minor: La, Pr, Nd, Ca and Al
Trace: Si, Ba, Mg and F

Numerous investigations have shown that the main feature of the highly productive polishing powder is the significant content of CeO_2 because the crystal structure has its own peculiarities, such as polishing ability, mechanical strength and wear resistance.[7,8] In addition, the production of new types of rare earth polishing material has begun to involve higher CeO_2 content in solid solutions of rare earth oxides. In addition, La, Pr and Nd, like Ce, are also used in polishing as well as dyes in glass.[9,10] In contrast, non-rare earth metals such as Ca, Al, Si, Ba, Mg and F account for some proportion of REPPW, depending on the type of polished material.

As the above composition data show REPPW should be thought of as a new source of rare earth elements because these elements are used in numerous fields such as optical, permanent magnet, electronics, superconductor, hydrogen storage, medical and nuclear technologies, for which demand for these elements has been increasing.[9,10] Moreover, rare earth concentrates or ores are found in only a few countries and thus must often be imported. To preserve these elements, the investigation of rare earth recovery from REPPW is required, even though most of them have been buried in landfill because they are not easy to treat chemically or physically. A few studies involving rare earth metal recovery from REPPW by a hydrometallurgical method including ion exchange, solvent extraction, electrolysis and leaching have already been carried out.[2,6,11,12]

The leaching process using sulfuric acid solutions, which has been used industrially for the extraction of rare earths from ores and concentrates, can be proposed as a process for the recovery of rare earths from REPPW because it is easy and inexpensive to implement the treatment of REPPW. However, it also has some demerits in terms of separation and recovery. Undesired species are dissolved along with the materials of interest in the solution and another method is needed to separate these materials. For example, in the case of REPPW, there is difficulty in terms of purification from polished materials containing non-rare earth metal ions (Al^{3+}, Ca^{2+}, etc.) even if REPPW is dissolved by the leaching process.

For cerium recovery from REPPW by sulfuric acid leaching, therefore, it was suggested that there is s need to divide the leaching process into two steps based on the dissolution characteristics of the considered element-H_2SO_4–H_2O solutions. The two steps of the leaching process consist of case 1 with La_2O_3, Pr_2O_3, Nd_2O_3 and CaO and case 2 with CeO_2 and Al_2O_3. This classification can be useful for developing the total process for cerium recovery from REPPW via two-stage acid leaching based on experimental

*Corresponding author, E-mail: hiratou@energy.kyoto-u.ac.jp

results. In addition, a k-T (reaction rate constant-reaction temperature) diagram that permits rational extraction of CeO_2 and Al_2O_3 was devised according to the kinetics data fitted by a shrinking core model.

2. Experimental Methods

2.1 Materials

Lanthanum (III) oxide, praseodymium (III) oxide, neodymium (III) oxide, calcium (II) oxide and aluminum (III) oxide used in this study were of chemical grade of >99.9% metal basis (Sigma Aldrich, Ltd.) and all of them had <5 µm particle size.

2.2 Experimental methods

All experiments were carried out by putting the desired amount of each reagent into $0.1\,dm^3$ sulfuric acid solutions with various acid concentrations in a batch-type glass reactor of 300 mL heated at the desired temperature; the reactor was placed on a hot plate stirrer. The solution was stirred by a magnetic stirrer at the desired agitation speed. The dependent variables used in the experiments were as follows: sulfuric acid concentration and reaction temperature.

For measuring the weight of residual target oxide (i.e., La_2O_3, Pr_2O_3, Nd_2O_3 and CaO) and precipitated sulfate converted from target oxide vs. reaction time, the samples obtained at an appropriate reaction time were filtered from the solution on a 0.45 µm pore size membrane using a pressure filtration unit, and were washed 3 times using ethanol to remove the sulfuric acid. After drying at 45°C for 24 h, the weight (a) of the precipitate consisting of residual oxide and precipitated sulfate was measured using a balance. Then, the precipitate was added into water to dissolve the precipitated sulfate and residual oxide was recovered by filtration. The weight (b) of residual oxide was measured using a balance after drying at 45°C for 24 h. The difference between (a) and (b) reflected the weight of participated sulfate. In the case of Al_2O_3, only the initial weight (W_0) and residue (W_t) of target oxide after dissolution were measured to obtain data on the dissolution kinetics. The samples taken at different reaction times were filtered from the solution and washed using water to remove the sulfuric acid and dissolve the precipitated sulfate. After drying, the weight (W_t) of residual oxide was measured using a balance.

To identify the crystalline phases of precipitated sulfate, the obtained samples were measured using an X-ray diffractometer (PANalytical, X'pert PRO) for mineralogical analysis.

2.3 Kinetics analysis

The kinetics of the dissolution of CeO_2 in sulfuric acid solutions has already been reported by the author of this study.[13] It was found that the reaction rate for the dissolution of CeO_2 can be expressed by a shrinking core model that describes the fluid-solid reaction kinetics of dense (nonporous) particles.[14–17] Therefore, the experimental data of Al_2O_3 dissolution, which was performed under various sulfuric acid concentrations and reaction temperatures, were made to fit a shrinking core model to Al-dissolution vs. time curves. Assuming that the reaction rate of Al_2O_3 dissolution

was controlled by the surface chemical reaction and particles were in a homogeneous spherical solid phase, the data were analyzed using a model as follows:

$$1 - (1 - X_t)^{1/3} = kt. \tag{1}$$

Here, k is the reaction rate constant (h^{-1}) of the dissolution and X_t is the dissolved fraction vs. time t, which was then calculated as follows:
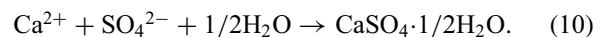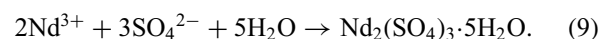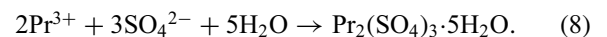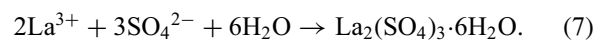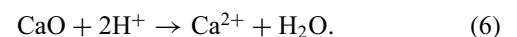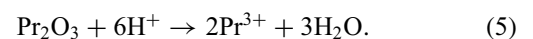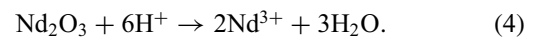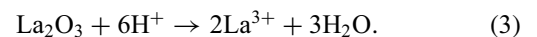
$$X_t = 1 - W_t/W_0. \tag{2}$$

Here, W_0 and W_t represent the initial and residual weights of Al_2O_3 vs. time t, respectively.

3. Results and Discussion

3.1 Precipitation of La, Pr, Nd and Ca sulfates converted from La_2O_3, Pr_2O_3, Nd_2O_3 and CaO in sulfuric acid solutions

The conversion kinetics of La_2O_3, Pr_2O_3, Nd_2O_3 and CaO with <5 µm particle size into La, Pr, Nd and Ca sulfates in sulfuric acid solutions was studied. Initial sulfuric acid concentration and reaction temperature were kept constant at $3\,mol/dm^3$ and 90°C, respectively. In addition, the initial amount of La_2O_3, Pr_2O_3, Nd_2O_3 and CaO per sulfuric acid solution was $0.08\,mol/dm^3$. The results are given in Fig. 1. The results show that the dissolution of La, Pr, Nd and Ca oxides occurred rapidly and it took less than 1 min for them to dissolve in acid solutions; under high solid-to-liquid ratio, the concentration of dissolved La^{3+}, Nd^{3+}, Pr^{3+} and Ca^{2+} exceeds the solubility and these cations directly form sulfate. The results of the XRD patterns shown in Fig. 2 provide evidence for that conversion. The chemical reactions below (eqs. (3)–(10)) are considered to be involved in the conversion of target oxide into precipitated sulfate in sulfuric acid solutions:

$$La_2O_3 + 6H^+ \rightarrow 2La^{3+} + 3H_2O. \tag{3}$$

$$Nd_2O_3 + 6H^+ \rightarrow 2Nd^{3+} + 3H_2O. \tag{4}$$

$$Pr_2O_3 + 6H^+ \rightarrow 2Pr^{3+} + 3H_2O. \tag{5}$$

$$CaO + 2H^+ \rightarrow Ca^{2+} + H_2O. \tag{6}$$

$$2La^{3+} + 3SO_4^{2-} + 6H_2O \rightarrow La_2(SO_4)_3 \cdot 6H_2O. \tag{7}$$

$$2Pr^{3+} + 3SO_4^{2-} + 5H_2O \rightarrow Pr_2(SO_4)_3 \cdot 5H_2O. \tag{8}$$

$$2Nd^{3+} + 3SO_4^{2-} + 5H_2O \rightarrow Nd_2(SO_4)_3 \cdot 5H_2O. \tag{9}$$

$$Ca^{2+} + SO_4^{2-} + 1/2H_2O \rightarrow CaSO_4 \cdot 1/2H_2O. \tag{10}$$

The formation of precipitated sulfate in the considered element-H_2SO_4–H_2O solutions, depending on the conditions of sulfuric acid concentration and temperature, may yield various forms: La, Pr and Nd sulfates absorb water, forming hydrates such as dihydrate, pentahydrate, hexahydrate, octahydrate and nonahydrate, and Ca has the forms of calcium sulfate dihydrate (gypsum, $CaSO_4 \cdot 2H_2O$), calcium sulfate hemi-hydrate ($CaSO_4 \cdot 1/2H_2O$), and calcium sulfate anhydrite ($CaSO_4$). The various crystal structures of sulfate hydrate as mentioned above have been the focus of much research, such as on crystal growth and solid state chemistry; however in this study, only the solubility and the precipitation degrees for target metal in the removal or recovery phase are important factors. Therefore, the precipitation behavior
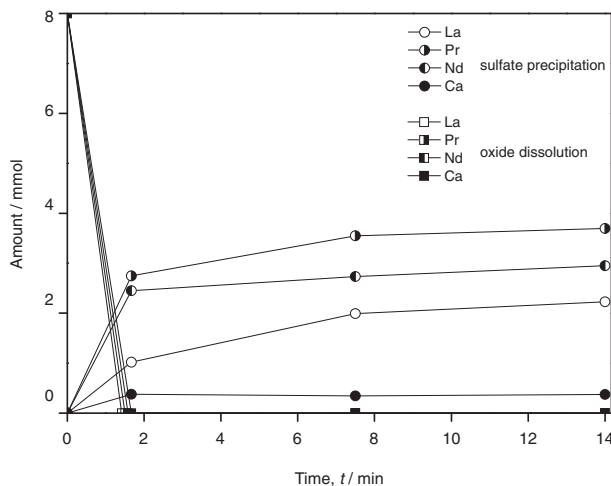
Fig. 1 Conversion kinetics of La_2O_3, Pr_2O_3, Nd_2O_3 and CaO into La, Pr, Nd and Ca sulfates in sulfuric acid solutions (90°C reaction temperature, 3 mol/dm³ sulfuric acid concentration and 0.08 mol/dm³ initial amount of La_2O_3, Pr_2O_3, Nd_2O_3 and CaO per sulfuric acid solution).
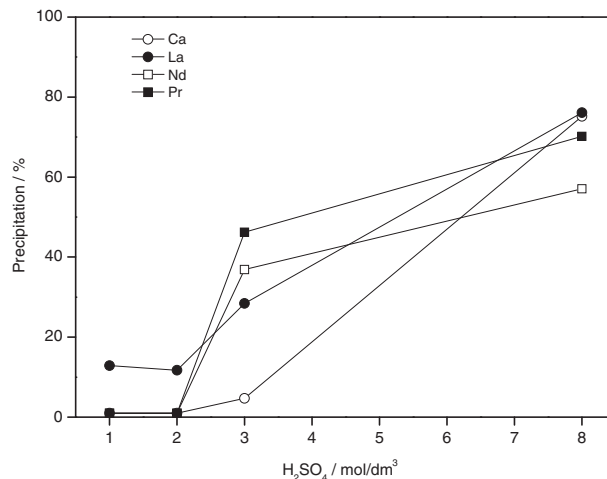

Fig. 3 Effect of sulfuric acid concentration on precipitation behavior of La, Pr, Nd and Ca sulfates converted from La_2O_3, Pr_2O_3, Nd_2O_3 and CaO in sulfuric acid solutions (90°C reaction temperature, 14 min reaction time and 0.08 mol/dm³ initial amount of La_2O_3, Pr_2O_3, Nd_2O_3 and CaO per sulfuric acid solution).
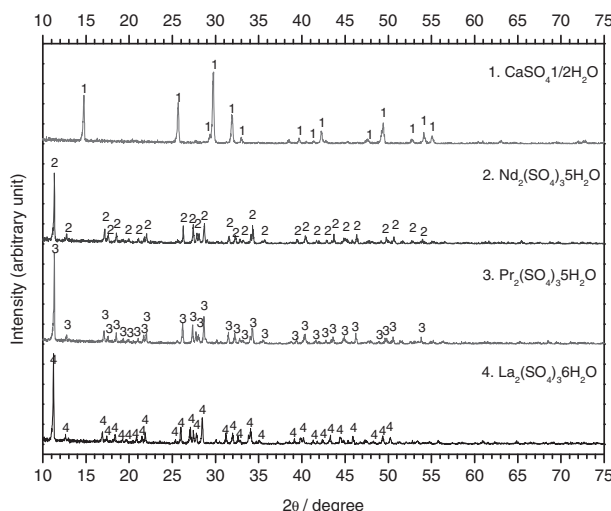

Fig. 2 XRD patterns of the precipitate obtained after 14 min reaction time (90°C reaction temperature, 3 mol/dm³ sulfuric acid concentration and 0.08 mol/dm³ initial amount of La_2O_3, Pr_2O_3, Nd_2O_3 and CaO per sulfuric acid solution).
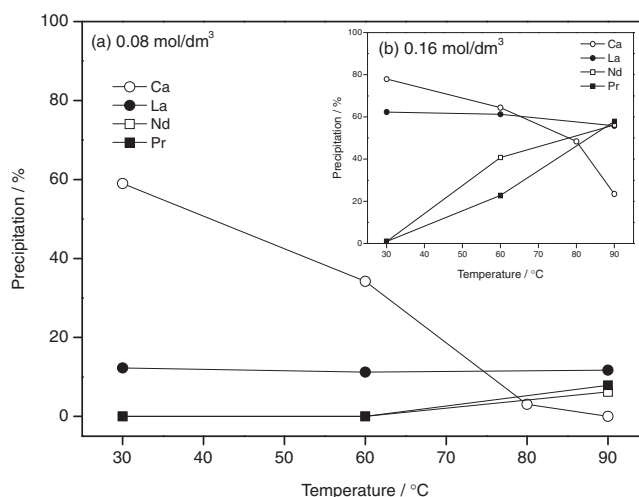

Fig. 4 Effect of reaction temperature on precipitation behavior of La, Pr, Nd and Ca sulfates converted from La_2O_3, Pr_2O_3, Nd_2O_3 and CaO in sulfuric acid solutions (2 mol/dm³ sulfuric acid concentration, 14 min reaction time and 0.08 (a) and 0.16 (b) mol/dm³ initial amount of La_2O_3, Pr_2O_3, Nd_2O_3 and CaO per sulfuric acid solution).

of La, Pr, Nd and Ca sulfates at various sulfuric acid concentrations and reaction temperatures was investigated.

The effect of sulfuric acid concentration, in the range from 1 to 8 mol/dm³, on the precipitation behavior of La, Pr, Nd and Ca sulfates converted from La_2O_3, Pr_2O_3, Nd_2O_3 and CaO in sulfuric acid solutions at 90°C reaction temperature after 14 min reaction time was studied and the initial amount of each target oxide per sulfuric acid solution was 0.08 mol/dm³. Figure 3 shows that increasing sulfuric acid concentration increased the precipitation by the well-known "common ion effect" and increasing SO_4^{2-} ion concentration led to decreased solubility of La, Pr, Nd and Ca sulfates.

In addition, La, Pr, Nd and Ca sulfates were precipitated using 2 mol/dm³ acid concentration at various temperatures ranging from 30 to 90°C after 14 min reaction time to

examine the effect of the reaction temperature. The initial amount of La_2O_3, Pr_2O_3, Nd_2O_3 and CaO per sulfuric acid solution was 0.08 or 0.16 mol/dm³. Figure 4 illustrates the changes in precipitation behavior of La, Pr, Nd and Ca sulfates in acidic solutions at various temperatures. This result explains the increasing precipitation of Pr and Nd sulfates with increasing reaction temperature. Unlike Pr and Nd, La sulfate had no effect on increasing temperature. In the case of Ca sulfate, the precipitation decreased with increasing temperature, which is in agreement with literature results; the explanation for this behavior concerns the two equilibria given by $CaSO_4 \cdot xH_2O = Ca^{2+} + SO_4^{2-} + xH_2O$ and $HSO^- = H^+ + SO_4^{2-}$, wherein Ca sulfate solubility increased in response to a lowered sulfate concentration caused by a shift to the left with increasing temperature of the bisulfate equilibrium.[18]
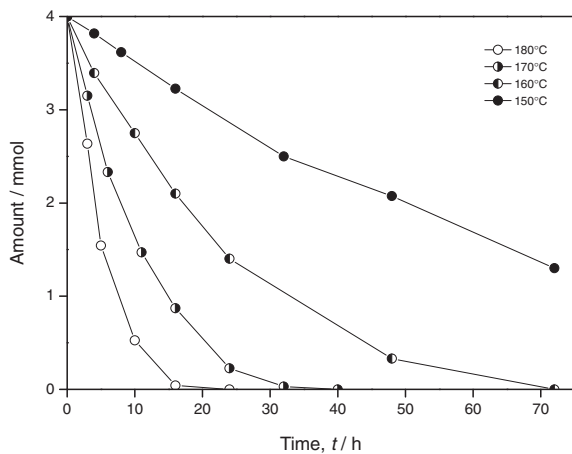
Fig. 5   Effect of reaction temperature on dissolution of Al_2O_3 in sulfuric acid solutions (14 mol/dm³ sulfuric acid concentration and 0.04 mol/dm³ initial amount of Al_2O_3 per sulfuric acid solution).
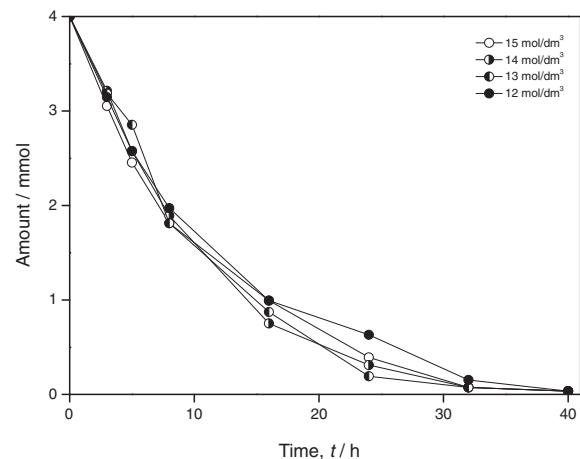

Fig. 6   Effect of sulfuric acid concentration on dissolution of Al_2O_3 in sulfuric acid solutions (170°C reaction temperature and 0.04 mol/dm³ initial amount of Al_2O_3 per sulfuric acid solution).

3.2   Dissolution kinetics of CeO_2 and Al_2O_3 in sulfuric acid solutions

The simple dissolution process of CeO_2 and Al_2O_3 in acid solutions can be described as follows:

$$CeO_2 + 4H^+ = Ce^{4+} + 2H_2O. \tag{11}$$

$$Al_2O_3 + 6H^+ = 2Al^{3+} + 3H_2O. \tag{12}$$
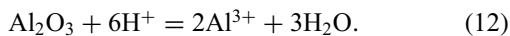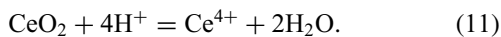
The dissolution kinetics depends on acid concentration and reaction temperature. On the basis of the above reactions, the effects of various acid concentrations and reaction temperatures were evaluated as described below.

According to Um et al.,[13] CeO_2 was very slowly dissolved in acid solutions; it took more than 48 h to dissolve 0.02 mol CeO_2 powder with 2.5 μm average particle size completely in 0.1 dm³ sulfuric acid solutions (8 mol/dm³) at 125°C. The dissolution rate of CeO_2 increased with increasing reaction temperature in the range from 105 to 135°C and increasing sulfuric acid concentration in the range from 8 to 12 mol/dm³. Al_2O_3 was also dissolved in 14 mol/dm³ sulfuric acid at different reaction temperatures of 150, 160, 170 and 180°C to examine the effect of reaction temperature on the dissolution rate, as shown in Fig. 5. The dissolution of Al_2O_3 was quite slow, even in such a highly concentrated acid. At 150°C, only 65% of Al_2O_3 was dissolved after the reaction for 3 d. The dissolution rate increased with increasing temperature, and Al_2O_3 could be completely dissolved in 24 h at 180°C. The effect of acid concentration on the dissolution rate was examined by using different acid concentrations of 12, 13, 14 and 15 mol/dm³ at 170°C. Unlike CeO_2, the acid concentration had a negligible effect on the dissolution rate, as shown in Fig. 6.

3.3   Study of cerium recovery from rare earth polishing powder waste (REPPW) via two-stage sulfuric acid leaching

The particle size distribution of REPPW summarized by Kim et al.[2] and Hoshino et al.[19] showed that D_{50}/μm was 1.689 and all particles were <5 μm. In addition, CeO_2, which is the main component of polishing materials, had an average particle diameter of 80 nm, which did not change even after

polishing. Besides, the particles that were bigger than CeO_2 were assigned to polished objects. Assuming that REPPW contains only Ce, La, Pr, Nd, Ca and Al materials (major and minor components as referred to in the introduction section) with <5 μm particle size as mentioned above, and organic materials remained in the surfactant and water, it is necessary to apply treatment using a calcination process for removal of organic material and oxidation of inorganic material. According to Yoon et al.,[6] TG results of REPPW showed that there were two clear and closely grouped mass change peaks for 100–150 and 150–500°C. The first weight loss between 100 and 150°C where the curve rapidly dropped was probably related to the decomposition of a hydrate and water. The second weight loss between 150 and 500°C was probably related to the decomposition of organic material and the oxidation of inorganic material. Therefore, when the REPPW is treated using a calcination process with a temperature of at least 500°C, the remaining residue will contain CeO_2, La_2O_3, Pr_2O_3, Nd_2O_3, CaO and Al_2O_3 with <5 μm particle size. The dissolution data presented in Figs. 1, 3, 4, 5 and 6 suggest the benefit of applying a two-step process for separation of La, Pr, Nd and Ca as by-products by leaching (case 1) and then recovery of Ce from the mixture of CeO_2 and Al_2O_3 by leaching (case 2). Figure 7 outlines the total process including leaching (case 1) and leaching (case 2), which is discussed in detail below.

3.3.1   Leaching (case 1)

In the case of leaching (case 1) shown in Fig. 7, La, Pr, Nd and Ca sulfates can appear as undesirable by-products, mostly as discarded solids, and disturb the recovery of cerium in the next leaching step (case 2) because the precipitated sulfate after the first leaching step (case 1) may be dissolved in solutions during subsequent leaching (case 2). Therefore, the change in precipitation of La, Pr, Nd and Ca sulfates according to sulfuric acid solution and reaction temperature was evaluated to remove La, Pr, Nd and Ca effectively during the initial leaching (case 1). As shown in Fig. 3, the precipitation of La, Pr, Nd and Ca sulfates at various acid concentrations was minimal at acid concentrations below 2 mol/dm³. It is clear that the measured precipitation curves
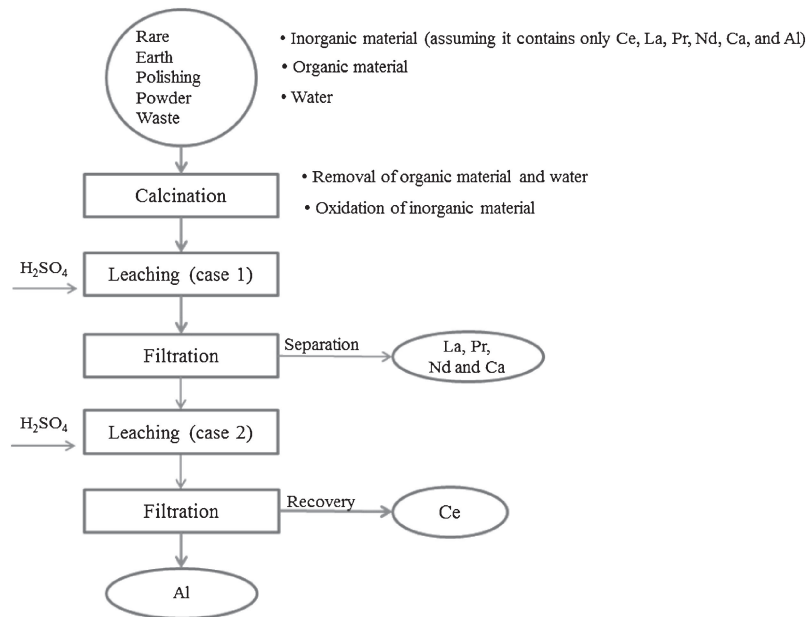
Fig. 7   Schematic flow diagram for hydrometallurgical treatment of rare earth polishing powder waste for recovery of cerium.
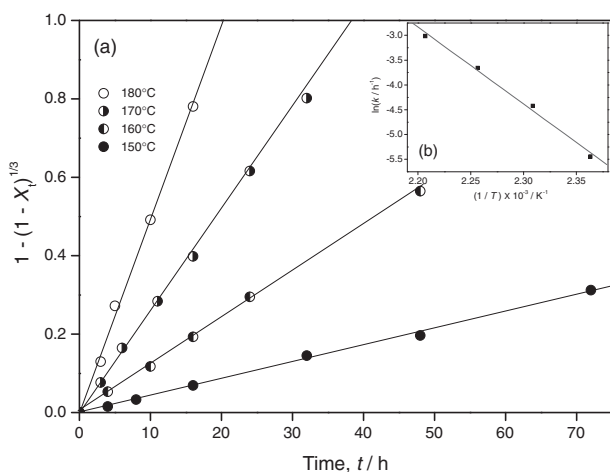

Fig. 8   Plots of $1 - (1 - X_t)^{1/3}$ versus reaction time for different reaction temperatures on dissolution of Al₂O₃ (a), and effect of reaction temperature on dissolution rate constants of Al₂O₃ (b).
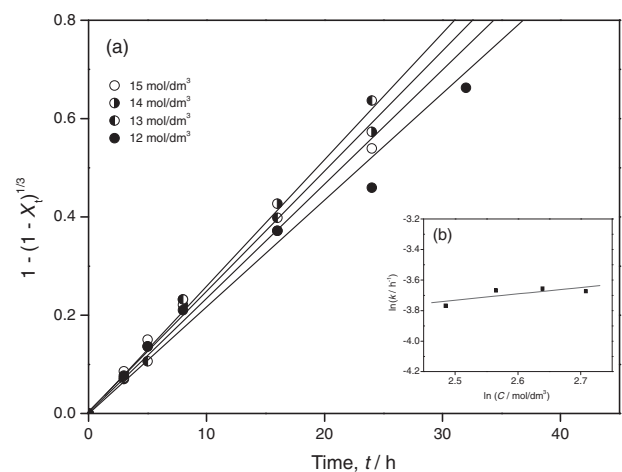

Fig. 9   Plots of $1 - (1 - X_t)^{1/3}$ versus reaction time for different sulfuric acid concentrations on dissolution of Al₂O₃ (a), and effect of sulfuric acid concentration on dissolution rate constants of Al₂O₃ (b).

were proportional to the acid concentration. Meanwhile, the same ranges of reaction temperature for minimizing precipitation of La, Pr, Nd and Ca sulfates did not produce clear results, as shown in Fig. 4. However, according to these data, it was possible to check whether the technologically interesting minimum of sulfate precipitation could be found by a rather simple calculation for factors such as initial amount of target oxide per sulfuric acid solution, sulfuric acid concentration and reaction temperature in leaching (case 1).

3.3.2   Leaching (case 2)

After the separation of La, Pr, Nd and Ca in leaching (case 1), the residue mainly contained CeO₂ and Al₂O₃. Following kinetics data of CeO₂ and Al₂O₃ dissolution, cerium and aluminum could be separated by leaching (case 2). In the case of CeO₂, the kinetics data calculated by Um *et al.*[13] was used in this study. The kinetics data of Al₂O₃ dissolution performed under various conditions of

sulfuric acid concentration and reaction temperature, as shown in Figs. 5 and 6, were calculated as follows.

As shown in Figs. 8(a) and 9(a), $1 - (1 - X_t)^{1/3}$ plotted against reaction time t is almost a straight line for each experimental condition, with a correlation coefficient of more than 0.99, indicating that the dissolution data reasonably followed a shrinking core model. The rate constant k varies with experimental conditions and is the function of reaction temperature and sulfuric acid concentration. When CeO₂ and Al₂O₃ were dissolved into sulfuric acid solutions in all experiments, the dissolution rate constant considered as a function of reaction temperature and sulfuric acid concentration can be expressed by the following equation:

$$k = k_0' e^{-E_a/RT} C^m. \tag{13}$$

Here, E_a is the activation energy (kJ/mol); R, the ideal gas constant, 8.314×10^{-3} (kJ/mol K); T, the reaction temper-

ature (K); C, sulfuric acid concentration (mol/dm³); k_0', pre-exponential factor; and m is a constant. As for the dissolution of CeO_2, the following equation was obtained:[13]

$$k = 1.4268 \times 10^8 e^{-14831/T} C^{6.54}. \quad (14)$$

Linear regressions in Figs. 8(a) and 9(a) were used to calculate k values from the slopes. In addition, the $\ln k$ values calculated from these k values were plotted against $1/T$ and $\ln C$ using equations $k = k_1' e^{-E_a/RT}$ and $k = k_2' C^m$, where k_1' and k_2' are the pre-exponential factors. The activation energy and m were calculated from the slopes of the lines in Figs. 8(b) and 9(b), respectively.

Figure 8(a) shows the effect of reaction temperature on dissolution rate. The slopes of the experimental data in Fig. 8(a) were used to determine the reaction rate constants for various temperatures in the dissolution stage. As shown in Fig. 8(b), the increase in dissolution rate constant of Al_2O_3 with increasing temperature obeyed the Arrhenius equation with an activation energy of 130 kJ/mol. The slopes in Fig. 9(a) were used to determine the reaction rate constant related to the sulfuric acid concentration. Plots of $\ln k$ versus $\ln C$ in Fig. 9(b) show that the constant (m) of Al_2O_3 was calculated to be 0.41. The large constant of 6.54 indicates a strong effect of acid concentration on the dissolution rate of CeO_2, whereas Al_2O_3 has less effect on the dissolution rate owing to changing acid concentration. The kinetics equation on dissolution of Al_2O_3 was $k = 1.2299 \times 10^{13} e^{-15482/T} C^{0.41}$.

Rearranging eq. (13), one obtains

$$\ln k = -(E_a/R)1/T + (\ln k_0' + m \ln C). \quad (15)$$

Putting the calculated $k_0' = 1.4268 \times 10^8$ (CeO_2) and $k_0' = 1.2299 \times 10^{13}$ (Al_2O_3) into eq. (15), the expressions between $\ln k$ and $1/T$ at various acid concentrations (C) can be obtained as follows.

$(1/T) \times 10^3$ from 2.1 to 3.1, here C is 8:

$$CeO_2: \ln k = -14831/T + 32.3757. \quad (16)$$

$$Al_2O_3: \ln k = -15482/T + 30.9931. \quad (17)$$

Here C is 10:

$$CeO_2: \ln k = -14831/T + 33.8350. \quad (18)$$

$$Al_2O_3: \ln k = -15482/T + 31.0846. \quad (19)$$

Here C is 12:

$$CeO_2: \ln k = -14831/T + 35.0274. \quad (20)$$

$$Al_2O_3: \ln k = -15482/T + 31.1593. \quad (21)$$

Here C is 14:

$$CeO_2: \ln k = -14831/T + 36.0356. \quad (22)$$

$$Al_2O_3: \ln k = -15482/T + 31.2225. \quad (23)$$

The revised k-T diagram for a CeO_2–Al_2O_3–H_2SO_4–H_2O system can then be constructed as shown in Fig. 10 using the expressions given previously; the boiling points of H_2SO_4–H_2O solutions at different acid concentrations of 8, 10, 12 and 14 mol/dm³ were calculated using OLI® software. The devised k-T diagram can be used to predict the dissolution behavior between CeO_2 and Al_2O_3 in leaching (case 2) of a schematic flow diagram (Fig. 7). For example, CeO_2 can be dissolved leaving Al_2O_3 in a stable solid phase under dissolution conditions calculated using this diagram; the
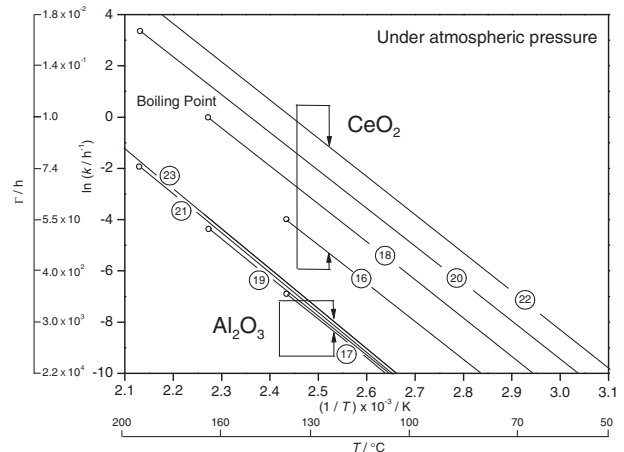

Fig. 10   Revised k-T diagram for CeO_2–Al_2O_3–H_2SO_4–H_2O system.

increasing difference in τ (time for complete dissolution reaction (h) = $e^{-\ln k}$) between cerium and aluminum in the diagram leads CeO_2 to be separated from Al_2O_3 almost completely by leaching (case 2).

3.3.3 Lab-scale experiment of cerium recovery from the mixture of CeO_2, La_2O_3, Pr_2O_3, Nd_2O_3, CaO and Al_2O_3 via two-stage sulfuric acid leaching

The cerium separation from the mixture of 23.2 g of CeO_2 (46.4 mass%), 13.9 g of La_2O_3 (27.8%), 1.5 g of Pr_2O_3 (3.0%), 2.6 g of Nd_2O_3 (5.2%), 3.1 g of CaO (6.2%) and 5.7 g of Al_2O_3 (11.4%) was tested according to the studied hydrometallurgical treatment shown in Fig. 7. For the minimum of La, Pr, Nd and Ca sulfate precipitation after dissolution, the conditions of first-stage leaching were fixed for 2 mol/dm³ sulfuric acid solutions at 50 g/dm³ initial amount of the mixture per sulfuric acid solution, 650 rpm agitation rate, 14 min reaction time and 90°C reaction temperature using the composition of sample and the data shown in Figs. 3 and 4. The resulting residue after leaching was found to contain 23.2 g of CeO_2, 5.7 g of Al_2O_3, 0.06 g of $La_2(SO_4)_2 \cdot 6H_2O$ and 0.16 g of $CaSO_4 \cdot 1/2H_2O$. Next, in order to recover cerium from the residue, second-stage leaching was carried out with a 12 mol/dm³ sulfuric acid concentration and 28.9 g/dm³ initial amount of the residue per sulfuric acid solution, 650 rpm agitation rate, 36 h reaction time and 120°C temperature. After leaching, the leaching solution was diluted from 12 to 3–4 mol/dm³ using water for dissolution of $Ce(SO_4)_2$ precipitate converted from CeO_2 in sulfuric acid solutions. The filtrate of diluted solutions showed that the concentration of dissolved cerium was 18.9 g/dm³, containing less than 90 ppm of other impurities such as La ($<$30 ppm), Ca ($<$50 ppm) and Al ($<$10 ppm). In addition, the only powder left behind in the filtrate was 5.7 g of Al_2O_3.

4. Conclusion

This research focused on the leaching of CeO_2, La_2O_3, Pr_2O_3, Nd_2O_3, CaO and Al_2O_3, which are the main elements of rare earth polishing powder waste (REPPW), for a study of cerium recovery from REPPW by a hydrometallurgical process. This involved a two-stage leaching process in series with sulfuric acid solutions, which was efficient to dissolve

the main elements selectively and then to recover cerium. Each dissolution experiment of case 1 with La$_2$O$_3$, Pr$_2$O$_3$, Nd$_2$O$_3$ and CaO and case 2 with CeO$_2$ and Al$_2$O$_3$ by means of two-stage leaching was studied in terms of the optimal conditions, and the obtained results are explained as follows:

(1) Leaching (case 1): La$_2$O$_3$, Pr$_2$O$_3$, Nd$_2$O$_3$ and CaO in 1–8 mol/dm^3 sulfuric acid solutions at 30–90°C temperature were dissolved in less than 1 min and then dissolved cations in acid solutions directly formed La, Pr, Nd and Ca sulfates because their concentrations exceeded their solubility. The precipitation ratio of Pr and Nd sulfates increased with increasing temperature, whereas that of Ca sulfate increased with decreasing temperature and La was not affected by temperature. Increasing acid concentration increased the precipitation of all sulfates.

(2) Leaching (case 2): Al$_2$O$_3$ in 12–15 mol/dm^3 acid concentration at 150–180°C was dissolved quite slowly, even with such highly concentrated acid and high temperature. Increasing temperature increased the dissolution rate of Al$_2$O$_3$, whereas the dissolution rate was negligibly affected by acid concentration.

These results suggested the benefit of using two leaching processes for separation of La, Pr, Nd and Ca by leaching (case 1) and then cerium recovery from a residual mixture of CeO$_2$ and Al$_2$O$_3$ by leaching (case 2). On the basis of the experimental results of leaching cases 1 and 2, the total process for cerium recovery from REPPW via two-stage acid leaching was developed.

The dissolution kinetics of Al$_2$O$_3$ in sulfuric acid solutions was also investigated and the experimental data were fitted by a shrinking core model. The activation energy of Al$_2$O$_3$ was 130 kJ/mol and the dissolution rate constant can be expressed as a function of reaction temperature and acid concentration as $k = 1.2299 \times 10^{13} e^{-15482/T} C^{0.41}$. Using the obtained functions, the k-T (reaction rate constant-reaction temperature) diagram for a CeO$_2$–Al$_2$O$_3$–H$_2$SO$_4$–H$_2$O system that predicts the dissolution behavior of CeO$_2$ and Al$_2$O$_3$ was devised and could be useful for cerium separation in leaching (case 2).

REFERENCES

1) X. Tao and P. Huiqing: J. Rare Earths **27** (2009) 1096–1102.
2) J. Y. Kim, U. S. Kim, M. S. Byeon, W. K. Kang, K. T. Hwang and W. S. Cho: J. Rare Earths **29** (2011) 1075–1078.
3) X. Y. Wang, J. M. Liu, Q. S. Yang, J. Du, F. E. Wang and W. Tao: J. Therm. Anal. Calorim. **109** (2012) pp. 419–424.
4) S. Chong, D. Holmstrom, Q. Li and T. Ouyang: VATTEN **65** (2009) 193–200.
5) K. Kato, T. Yoshioka and A. Okuwaki: Ind. Eng. Chem. Res. **39** (2000) 943–947.
6) H. S. Yoon, C. J. Kim, S. D. Kim, J. Y. Lee, S. W. Cho and J. S. Kim: J. Korean Inst. Resources Recycl. **12** (2003) 10–15.
7) R. Sabia, H. J. Stevens and F. R. Varner: J. Non-Cryst. Solids **249** (1999) 123–130.
8) N. S. Ong and V. C. Venkatesh: Mater. Process. Technol. **83** (1998) 261–266.
9) C. K. Gupta and N. Krishnamurthy: *Extractive Metallurgy of Rare Earths*, (CRC PRESS, New York, 2005).
10) British Geological Survey developed by BGS©NERC http://www.mineralsuk.com.
11) H. S. Yoon, C. J. Kim, H. C. Eom and J. S. Kim: J. Korean Inst. Resources Recycl. **14** (2005) 3–9.
12) T. Ozaki, K. I. Machida and G. Y. Adachi: Metall. Mater. Trans. B **30** (1999) 45–51.
13) N. Um and T. Hirato: Mater. Trans. **53** (2012) 1986–1991.
14) D. Georgiou and V. G. Papangelakis: Hydrometallurgy **49** (1998) 23–46.
15) M. Özdemir and H. Çetişli: Hydrometallurgy **76** (2005) 217–224.
16) E. A. Abdel-Aal and M. M. Rashad: Hydrometallurgy **74** (2004) 189–194.
17) S. Qiu, C. Wei, M. Li, X. Zhou, C. Li and Z. Deng: Hydrometallurgy **105** (2011) 350–354.
18) F. E. Farrah, G. A. Lawrance and E. J. Wanless: Hydrometallurgy **86** (2007) 13–21.
19) T. Hoshino, Y. Kurata, Y. Terasaki and K. Susa: J. Non-Cryst. Solids **283** (2001) 129–136.